# Membrane Topology of Helices VII and XI in the Lactose Permease of *Escherichia coli* Studied by *lacY*−*phoA* Fusion Analysis and Site-Directed Spectroscopy

M. L. Ujwal,[‡,§] Heinrich Jung,[‡,∥] Eitan Bibi,[‡,⊥] Colin Manoil,[#] Christian Altenbach,[○] Wayne L. Hubbell,[○] and H. Ronald Kaback*[,‡]

*Howard Hughes Medical Institute, Departments of Physiology and of Microbiology and Molecular Genetics, Molecular Biology Institute, Jules Stein Eye Institute, and Department of Chemistry and Biochemistry, University of California, Los Angeles, Los Angeles, California 90095, and Department of Genetics, University of Washington, Seattle, Washington 98195*

*Received July 26, 1995; Revised Manuscript Received September 14, 1995*[⊗]

ABSTRACT: The use of lactose permease−alkaline phosphatase fusions (*lacY*−*phoA*) demonstrates that the lactose permease of *Escherichia coli* contains 12 transmembrane domains and that approximately half of a transmembrane domain is required to translocate alkaline phosphatase to the periplasmic surface of the membrane [Calamia, J., & Manoil, C. (1990) *Proc. Natl. Acad. Sci. U.S.A. 87*, 4937−4941]. We have now used fusion analysis in combination with site-directed spectroscopy to examine more precisely the topology of putative helices VII and XI which contain the interacting residues Asp237 and Lys358, respectively. For this purpose, alkaline phosphatase was fused to alternate amino acid residues in transmembrane domains VII and XI. A sharp increase in alkaline phosphatase activity is observed as the fusion junction proceeds from Tyr228 to Ile230 in helix VII and from Phe354 to Phe356 in helix XI, suggesting that these residues approximate the middle of the corresponding transmembrane helices. Analysis of fluorescence quenching of the pyrene-labeled single-Cys mutants Asp237→Cys or Lys358→Cys, as well as measurement of collision frequencies between freely diffusing paramagnetic probes and a nitroxide spin-label at these sites, also indicates that Asp237 and also Asp240, which interacts with Lys319 (helix X), are located in transmembrane domains. However, Asp237 and Asp240 are accessible both from the aqueous phase and from within the membrane. The results provide more direct evidence that the three residues are located within transmembrane helices and suggest that Asp237 and Asp240 are either located near the periplasmic surface of the membrane or exposed within a solvent-filled cleft in the permease.

The lactose (lac)[1] permease of *Escherichia coli* is a hydrophobic, polytopic cytoplasmic membrane protein that catalyzes the coupled translocation of β-galactosides and $H^+$ with a stoichiometry of unity (i.e., symport or cotransport). Encoded by the *lacY* gene, the permease has been solubilized from the membrane, purified, reconstituted into proteoliposomes, and shown to be solely responsible for β-galactoside transport in monomeric form [reviewed in Kaback (1989, 1992); see Sahin-Tóth et al. (1994) in addition]. Based on circular dichroism and hydropathy analysis of the primary amino acid sequence, a secondary structure model was proposed in which the protein consists of a short hydrophilic N-terminus, 12 hydrophobic domains in α-helical conformation that traverse the membrane in zigzag fashion connected by hydrophilic loops, and a 17 amino acid residue hydrophilic C-terminal tail (Foster et al., 1983) (Figure 1). Evidence supporting the general features of the model and demonstrating that both the N and C termini, as well as the loops between helices IV and V and between helices VI and VII, are on the cytoplasmic face of the membrane was obtained from other spectroscopic techniques, limited proteolysis, immunological studies, and chemical modification [reviewed in Kaback (1989, 1992)]. Moreover, Calamia & Manoil (1990) have provided unequivocal support for the topological predictions of the 12-helix model by analyzing an extensive series of lac permease−alkaline phosphatase (*lacY*−*phoA*) fusion proteins and demonstrated in addition that approximately half a transmembrane domain is required to translocate alkaline phosphatase across the membrane. Recently, a model describing helix packing in the C-terminal half of the permease has been proposed based on the combined use of site-directed excimer fluorescence, second-site suppressor analysis, and site-directed mutagenesis [Jung et al., 1993; reviewed in Kaback et al. (1993, 1994)].

Second-site suppressor analysis (King et al., 1991) demonstrated originally that Asp237, which was placed initially in the periplasmic loop between helices VII and VIII (Foster

* Author to whom correspondence should be addressed at HHMI/UCLA, 5-748 MacDonald Research Labs, Box 951662, Los Angeles, CA 90095-1662. Telephone: (310) 206-5053. Telefax: (310) 206−8623.

‡ Howard Hughes Medical Institute, University of California, Los Angeles.

§ Present address: Department of Molecular Biophysics and Biochemistry, Yale University, 266 Whitney Ave., P.O. Box 208114, New Haven, CT 06520-8114.

∥ Present address: Universität Osnabrück, Abteilung Mikrobiologie, Barbarastrasse 11, D-49069 Osnabrück, Germany.

⊥ Present address: Department of Biochemistry, Weizmann Institute, Rehovot 76100, Israel.

#University of Washington.

○ Jules Stein Eye Institute, University of California, Los Angeles.

⊗ Abstract published in *Advance ACS Abstracts,* November 1, 1995.

[1] Abbreviations: lac, lactose; IPTG, isopropyl 1-thio-β-D-galactopyranoside; $KP_i$, potassium phosphate; SDS, sodium dodecyl sulfate; BCIP, 5-bromo-4-chloro-5-indolyl phosphate; PM, *N*-(1-pyrenyl)-maleimide; methanethiosulfonate spin-label, *S*-(1-oxy-2,2,5,5-tetramethylpyrroline-3-methyl) methanethiosulfonate; NiAA, nickel(II) acetylacetonate; OG, octyl β-D-glucopyranoside; DTT, dithiothreitol; C-less permease, functional permease devoid of cysteine residues.

0006-2960/95/0434-14909$09.00/0 

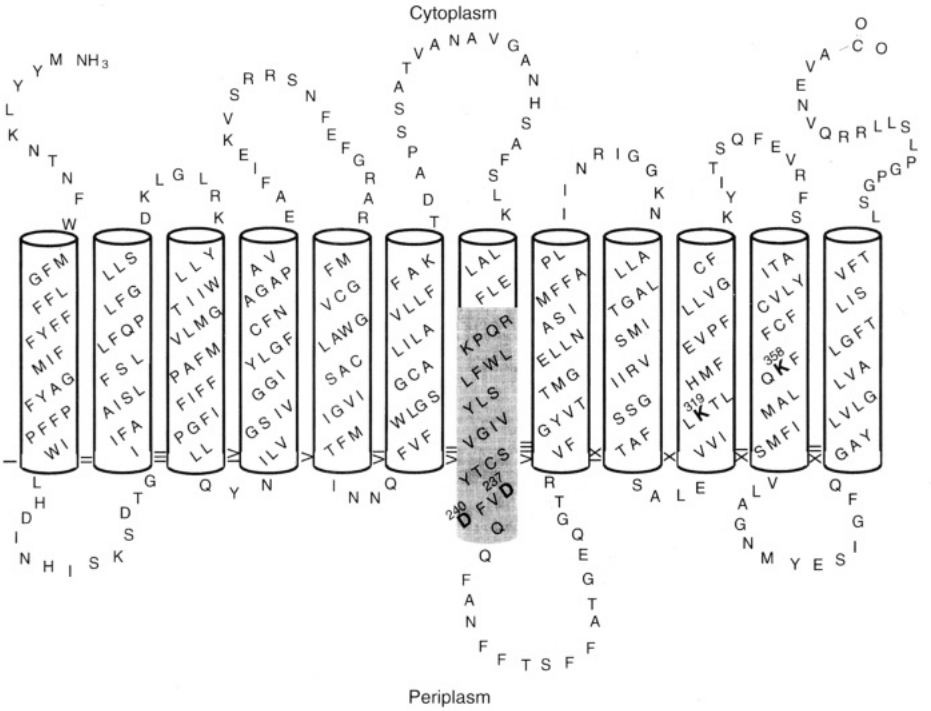


FIGURE 1: Secondary structure model of lactose permease. The model is based on the hydropathy plot of the primary sequence of the permease (Foster et al., 1983) and the modification of helix VII as suggested by the data presented in this paper. The single-letter amino acid code is used, 12 hydrophobic putative transmembrane helices are shown in boxes, and the shaded box represents the modified model. Sites of labeling with spin and fluorescence probes (Asp237, Asp240, and Lys358) are in boldface. Lys319 is also boldfaced, as it interacts functionally with Asp240.

et al., 1993), interacts with Lys358 (helix XI). As a result, it was suggested that the postulated secondary structure be altered in order to stabilize the putative salt bridge by placing residues 235 through 247 within helix VII, rather than the periplasmic loop between helices VII and VIII, and residues 222 through 210 in the cytoplasmic loop between helices VI and VII, rather than within helix VII (Figure 1). Subsequently, evidence for the interaction was confirmed and extended (Sahin-Tóth et al., 1992; Dunten et al., 1993; Sahin-Tóth & Kaback, 1993), and it was shown that Asp240 and Lys319 (helix X) also interact functionally (Sahin-Tóth et al., 1992; Lee et al., 1992; Sahin-Tóth & Kaback, 1993), although the nature of the interaction is different from that between Asp237 and Lys358. Recently, direct evidence that positions 237 and 358 are in close approximation has been obtained (Jung et al., 1995; He et al., 1995a,b). Permease containing His residues in place of Asp237 and Lys358 binds $Mn^{2+}$ stoichiometrically in a pH-dependent manner. On the other hand, permease with His residues in place of Asp240 and Lys319 does not bind metal.

In order to define the boundaries of transmembrane domain VII, Zen et al. (1994) studied functional complementation of lac permease fragments. The approach is based on the observation that contiguous, nonoverlapping permease fragments with discontinuities in hydrophilic loops form functional duplexes, while fragments with discontinuities in transmembrane domains do not. The results are consistent with the modified secondary structure model (King et al., 1991) in which Asp237 and Asp240 are contained within transmembrane domain VII rather than the periplasmic loop between helices VII and VIII (Figure 1).

The data presented here further define the topology of transmembrane domains VII and XI. Analysis is based on the alkaline phosphatase activity of a series of lac permease−alkaline phosphatase fusion proteins, as well as site-directed spectroscopic studies. The results support the argument that Asp237, Asp240, and Lys358 are located within transmembrane domains in an environment that is close to the aqueous phase.

## EXPERIMENTAL PROCEDURES

*Materials.* Isopropyl 1-thio-β-D-thiogalactoside (IPTG), 5-bromo-4-chloro-3-indolyl phosphate (BCIP; *p*-toluidine salt), and *p*-nitrophenyl phosphate were purchased from Sigma Chemical Co., St. Louis, MO. Bacterial alkaline phosphatase antibody (Anti-BAP) was from 5′Prime-3′Prime, Inc., Boulder, CO. Calf intestinal phosphatase was from Boehringer Mannheim GmbH, Mannheim, Germany. [1-$^{14}$C]Lactose was obtained from Amersham, Arlington Heights, IL. [$^{35}$S]Adenosine 5′-(α-thiotriphosphate) and [$^{35}$S]methionine were from New England Nuclear, Boston, MA. Oligonucleotides were synthesized on an Applied Biosystems DNA synthesizer. Gene Clean DNA purification kits were obtained from BIO 101 Inc., La Jolla, CA. Magic Mini Prep kits and immobilized monomeric avidin were purchased from Promega, Madison, WI. Purified *E. coli* phospholipids were purchased from Avanti, Alabaster, AL. Pyrene maleimide was from Molecular Probes (Eugene, OR). Nickel(II) acetylacetonate was obtained from Aldrich, Milwaukee, WI. *S*-(1-Oxy-2,2,5,5-tetramethylpyrroline-3-methyl) methanethiosulfonate (methanethiosulfonate spin-label) was a gift of Kálmán Hideg (University of Pécs, Hungary). Restriction enzymes, modification enzymes and all other materials were reagent grade and obtained from commercial sources.

*Bacterial Strains and Plasmids. E. coli* strains CC159 [F128 *lacI*$^q$ Δ(*ara, leu*) 7679 ΔlacX74 *phoA* Δ*20 galE galK*

*thi rpsE rpoB argE(am) recA1*] and CC181 [CC159 *lac Y328* (am)] were used to propagate plasmid pCM480 (Calamia & Manoil, 1990); pT7−5/*lacY* cassette (EMBL-X56095) and pT7−5(*lacY*−*phoA*) (this paper) encoding full-length *lacY* cassette fused in-frame at 3′ with the *phoA* gene. *E. coli* T184 [$lacI^+O^+Z^-Y^-(A)$, *rpsL*, $met^-$, $thr^-$, *recA*, *hsdM*, *hsdR*/*F*′, $lacI^qO^+Z^{D118}(Y^+A^+)$] (Teather et al., 1980) harboring plasmid pT7−5/C-less *lacY* L6XB [cassette *lacY* gene devoid of Cys codons (C-less; van Iwaarden et al., 1991) with a biotin acceptor domain in the middle cytoplasmic loop (Consler et al., 1993)] encoding given single-Cys mutants and plasmid pGP1−2 was used for overexpression of the mutant protein via the T7 promoter (Tabor & Richardson, 1985).

*Construction of Cassette lacY−phoA Fusion Plasmid pT7−5(lacY−phoA).* Plasmid pT7−5/*lacY* containing a cassette version of the *lacY* gene was linearized with restriction endonuclease *Esp*I, treated with calf intestinal alkaline phosphatase, and isolated on a 1% agarose gel and gene cleaned (Bio101). A 2.2 kb fragment obtained after digestion of plasmid pCM480 (Calamia & Manoil, 1990) with *Esp*I carrying the *phoA* gene was cloned into the *Esp*I site of plasmid pT7−5/*lacY* cassette. This results in a plasmid that has the *lacY* cassette gene and the *phoA* gene in tandem (Figure 2). A region after the 3′ end of *phoA* comprising a *Bst*EII−*Esp*I fragment of pCM480 and the *Esp*I−*Hin*dIII C-terminal fragment of *lacY* was then deleted by digestion with restriction endonucleases *Bst*EII and *Hin*dIII, Klenow end-filling, and religation of the plasmid. A unique *Nhe*I site was introduced at the fusion junction of *lacY* and *phoA* by a silent mutation at the first codon immediately after the *lacY* gene by the two-stage polymerase chain reaction (PCR) overlap extension method (Ho et al., 1989) using $Vent^R$ DNA polymerase. Additionally, in order to have a unique *Nde*I site within the fusion protein coding sequence, the second *Nde*I site in the vector sequence was destroyed by partial digestion, followed by Klenow end-filling and religation of blunt ends.

*Construction of Lac Permease−Alkaline Phosphatase (lacY−phoA) Gene Fusions.* Lac permease−alkaline phosphatase gene fusions were constructed using PCR with a sense primer complementary to the N terminus of *lacY* in combination with antisense primers complementary to the C termini of the desired *lacY* fragments (Table 1). The latter primers created a *Nhe*I site at the C termini of the different *lacY* fragments. The amplified fragments were digested with *Xho*I and *Nhe*I and then cloned into pT7−5(*lacY*−*phoA*) digested with the same two restriction enzymes. The *lacY*−*phoA* gene constructs were then propagated in *E. coli* CC181 (*phoA*$^-$) using LB plates containing ampicillin (100 μg/mL), spectinomycin (50 μg/mL), IPTG (2 mM), and BCIP (40 μg/mL). Desired gene fusions were identified by restriction analysis and finally sequencing of plasmid DNA isolated from cells of selected colonies (Sanger et al., 1977).

*Colony Morphology.* For preliminary qualitative assessment of alkaline phosphatase activity, transformed *E. coli* CC181 (*phoA*$^-$) were plated on indicator plates containing ampicillin (100 μg/mL), spectinomycin (50 μg/mL), IPTG (2 mM), and BCIP (40 μg/mL).

*Assay of Alkaline Phosphatase Activity. E. coli* CC181 harboring *lacY*−*phoA* fusion plasmids were cultivated in LB media at 37 °C. In the exponential growth phase, the cells were induced with 2 mM IPTG for 60 min. Alkaline phosphatase activity was assayed by measuring the rate of hydrolysis of *p*-nitrophenyl phosphate by permeabilized cells at 480 nm (Calamia & Manoil, 1990). Assays were performed in triplicate.

*Subcellular Fractionation.* Periplasmic proteins from *E. coli* CC181 were obtained by cold osmotic shock (Neu & Heppel, 1966). To prepare other cell fractions, spheroplasts were disrupted by sonication. The unbroken cells were removed by low-speed centrifugation, and membranes were harvested by ultracentrifugation at $200000g_{max}$ in a Beckman Optima TL ultracentrifuge. The supernatant was taken as the cytoplasmic fraction.

*[$^{35}$S]Methionine Labeling, Immunoprecipitation, and Electrophoresis.* Protein was immunoprecipitated from cell extracts after [$^{35}$S]methionine incorporation according to the protocol of Ito et al. (1981), except that heat treatment in the presence of SDS was carried out at 65 °C. Electrophoresis was performed as described (Manoil & Beckwith, 1985). Following electrophoresis, protein was detected and quantitated by Phosphor Imaging.

*Construction of Single-Cys Mutants.* Construction of the single-Cys mutants D237C/K358A[2] and D240C/K319A by site-directed mutagenesis has been described (Dunten et al., 1993; Sahin-Toth et al., 1992). A 0.3 kb DNA fragment encoding a biotin acceptor domain (Consler et al., 1993) was introduced at the unique *Xho*I site of the pT7−5/*lacY* cassette. Double-stranded DNA was sequenced by dideoxy chain termination (Sanger et al., 1977).

*Expression and Purification of Mutant Proteins.* Twelve liters of *E. coli* T184 cotransformed with pGP1−2 and pT7−5/*lacY* L6XB encoding given single-Cys mutants was cultivated at 30 °C and heat-shocked at 42 °C for 20 min. Membranes were prepared as described (Viitanen et al., 1986) and extracted with 1.25% octyl β-D-glucopyranoside (OG). The mutant protein was purified by affinity chromatography on immobilized monomeric avidin (Consler et al., 1993). The resin was equilibrated with 50 mM $KP_i$ (pH 7.5)/150 mM KCl/1.25% OG (w/v)/1 mM DTT/20 mM lactose/0.25 mg/mL of acetone/ether-washed *E. coli* phospholipids (column buffer). After application of the sample, the column was washed thoroughly with column buffer and, finally, with column buffer without DTT. Bound lac permease was then eluted with 8 mM *d*-biotin in column buffer without DTT. Purified samples were analyzed by SDS/polyacrylamide gel electrophoresis (Laemmli, 1970), followed by silver staining. Fractions containing purified permease were pooled.

*Fluorescent Labeling.* Labeling of single-Cys mutants with PM was performed as described (Jung et al., 1994). The modified protein was reconstituted into acetone/ether-washed *E. coli* phospholipids by detergent dilution (Viitanen et al., 1986). The protein:phospholipid ratio was adjusted to 1:385 (w/w). Proteoliposomes were centrifuged ($150000g_{max}$) and subsequently washed with 0.1% bovine serum albumin (w/v)/50 mM $KP_i$ (pH 7.5) and 4 times with 50 mM $KP_i$ (pH 7.5). Between washing steps, proteoliposomes were subject to two cycles of freeze−thaw/sonication. Proteoliposomes were finally resuspended in 50 mM $KP_i$ (pH 7.5). For each preparation, the amount of PM covalently

[2] Site-directed mutants are designated as follows: the one-letter amino acid code is used followed by a number indicating the position of the residue in wild-type lac permease. The sequence is followed by a second letter denoting the amino acid replacement at this position.

bound to the protein was determined by measuring the absorption of pyrene and calculating the concentration assuming an extinction coefficient of $2.2 \times 10^4$ $M^{-1}$ $cm^{-1}$ at 340 nm (Kouyama & Mihashi, 1981). Protein was determined using the amido-black method (Schaffner & Weissmann, 1973). The single-Cys mutants contained 0.6-0.8 mol of pyrene/mol of protein.

*Fluorescence Quenching.* Fluorescence spectra were recorded at 25 °C using an Aminco SLM 8000C spectrofluorometer equipped with a thermostated cell. Quenching experiments were performed using excitation at 344 nm with emission monitored at 378 nm. Aliquots of concentrated quencher solution were added to a suspension of proteoliposomes maintained at 25 °C with constant stirring. The solution of quencher and the proteoliposome suspension were saturated with argon before use. Values obtained were corrected for dilution. Quenching data were analyzed by Stern−Volmer plots where $F_0/F - 1$ is plotted against the concentration of quencher, [Q]. $F$ is the steady-state fluorescence intensity, and $F_0$ denotes fluorescence in the absence of quencher. A plot of $F_0/F - 1$ versus [Q] yields a slope equal to $K_{SV}$, the Stern−Volmer quenching constant. $K_{SV}$ is equal to the product of $k_q$, the bimolecular quenching constant, and $t_0$, the lifetime of pyrene in the absence of quencher.

*Spin Labeling.* Single-Cys mutants were modified with methanethiosulfonate spin-label by incubation of the purified, solubilized permease mutants with a 10-fold molar excess of spin-label in column buffer without DTT at 4 °C for 3 h. The modified protein was reconstituted into acetone/ether-washed *E. coli* phospholipids by detergent dilution as described above except that a protein:phospholipid ratio of 1:50 (w/w) was used.

*EPR Spectroscopy.* EPR spectra were recorded as described (Altenbach et al., 1989) on a Varian EPR spectrometer equipped with a loop gap resonator and a gas permeable TPX plastic sample capillary. The value of $\Delta P_{1/2}$, a quantity proportional to the collision frequency between a nitroxide bound to the protein and a paramagnetic species in solution, was determined for oxygen or nickel(II) acetylacetonate (NiAA) by power saturation spectroscopy (Altenbach et al., 1994).

*Protein Determination.* Protein was assayed by the method of Schaffner and Weissman (1973) with bovine serum albumin as standard.

## RESULTS

*Construction of lacY−phoA Gene Fusions.* Initially, the *phoA* gene excised from plasmid pCM480 (Calamia & Manoil, 1990) with restriction endonuclease *Esp*I was fused to the 3′ end of full-length cassette *lacY* gene in pT7−5 which was also digested with *Esp*I, yielding plasmid pT7−5(*lacY−phoA*) (Figure 2). In addition, a unique *Nhe*I site was generated at the junction between *lacY* and *phoA* by oligonucleotide-directed site-specific mutagenesis. Using this construct, DNA fragments encoding N-terminal permease fragments of desired size were amplified by PCR, thereby introducing a *Nhe*I site at the 3′ end using mutagenic primers listed in Table 1. The fragments were then fused to the *phoA* gene of pT7−5(*lacY−phoA*) by using the unique *Nhe*I site at the 5′ end of *phoA* and a second restriction site at the 3′ end of *lacY*. In this way, alkaline phosphatase was fused to alternate amino acid residues in transmembrane domains VII and XI. All fusions were verified by double-stranded DNA sequencing, and except for the base changes summarized in Table 1, the sequences were identical to those of cassette *lacY* and *phoA*.

*Colony Morphology.* Alkaline phosphatase activity of *lacY−phoA* fusions was assessed qualitatively by transforming *E. coli* CC181 (*phoA*⁻) with plasmid pT7−5(*lacY−phoA*) fusion derivatives and growing the transformants on indicator plates containing 5-bromo-4-chloro-5-indolyl phosphate (BCIP). Cells expressing active alkaline phosphatase hydrolyze BCIP and appear as dark blue colonies. In contrast, pale blue colonies are obtained with cells expressing fusions with low phosphatase activity. Cells expressing alkaline phosphatase fused at Leu216 to Tyr228 in putative transmembrane domain VII appear as pale blue colonies, whereas fusions to Ile230 to Gly254 in the same domain and the adjacent periplasmic loop grow as dark blue colonies. Alkaline phosphatase fusions at Val352 and Phe354 in putative transmembrane domain XI yield white and slightly blue colonies, respectively, while fusions at Phe356, Phe357, Lys358, or Tyr373 result in dark blue colonies.

*Alkaline Phosphatase Activity.* The alkaline phosphatase activity of cells expressing the *lacY−phoA* gene fusions was analyzed by measuring the hydrolysis of *p*-nitrophenyl phosphate. The activity profile of the fusions in helix VII (Figure 3A) clearly shows that the enzyme activities can be grouped into two distinct classes: (i) low-activity fusions comprising Leu216-PhoA[3] to Tyr228-PhoA; and (ii) high-activity fusions comprising Ile230-PhoA to Gly252-PhoA. Thus, moving from the cytoplasmic to the periplasmic face of putative transmembrane domain VII, a sharp increase in alkaline phosphatase activity is observed between Tyr228-PhoA and Ile230-PhoA. Assuming that half of the helix is required for the export of the alkaline phosphatase moiety (Calamia & Manoil, 1990), it seems likely that Tyr228 and Ile230 approximate the middle of transmembrane helix VII (Figure 1). Similarly, the activity profile of gene fusions in transmembrane domain XI (Figure 3B) clearly shows a sharp discontinuity between Phe354-PhoA and Phe356-PhoA, suggesting that these residues are probably at the approximate middle of the transmembrane domain.

*Expression and Stability of Fusion Proteins.* Rates of synthesis of the chimeric proteins were analyzed by [$^{35}$S]-methionine labeling of a representative set of fusions that cover both low and high alkaline phosphatase activity constructs. Chimeric proteins were identified by immunoprecipitation with anti-BAP, and representative data are presented in Figure 4. The relative molecular weight ($M_r$) of the chimeras is consistently smaller than predicted, as observed for the permease itself [see Viitanen et al. (1986)]. The intensity of each chimeric band (Figure 4, indicated by the arrows) was quantitated by Phosphor Imaging, and relative amounts of protein were determined (Table 2). With exception of Arg218-PhoA, no dramatic differences are observed between fusions exhibiting low or high alkaline phosphatase activity. Based on the relative amounts of protein, specific activities were calculated (Table 2), and the

[3] Lactose permease−alkaline phosphatase fusions are designated by the three-letter code of the C-terminal amino acid residue of the lac permease moiety followed by its position in the permease and -PhoA.

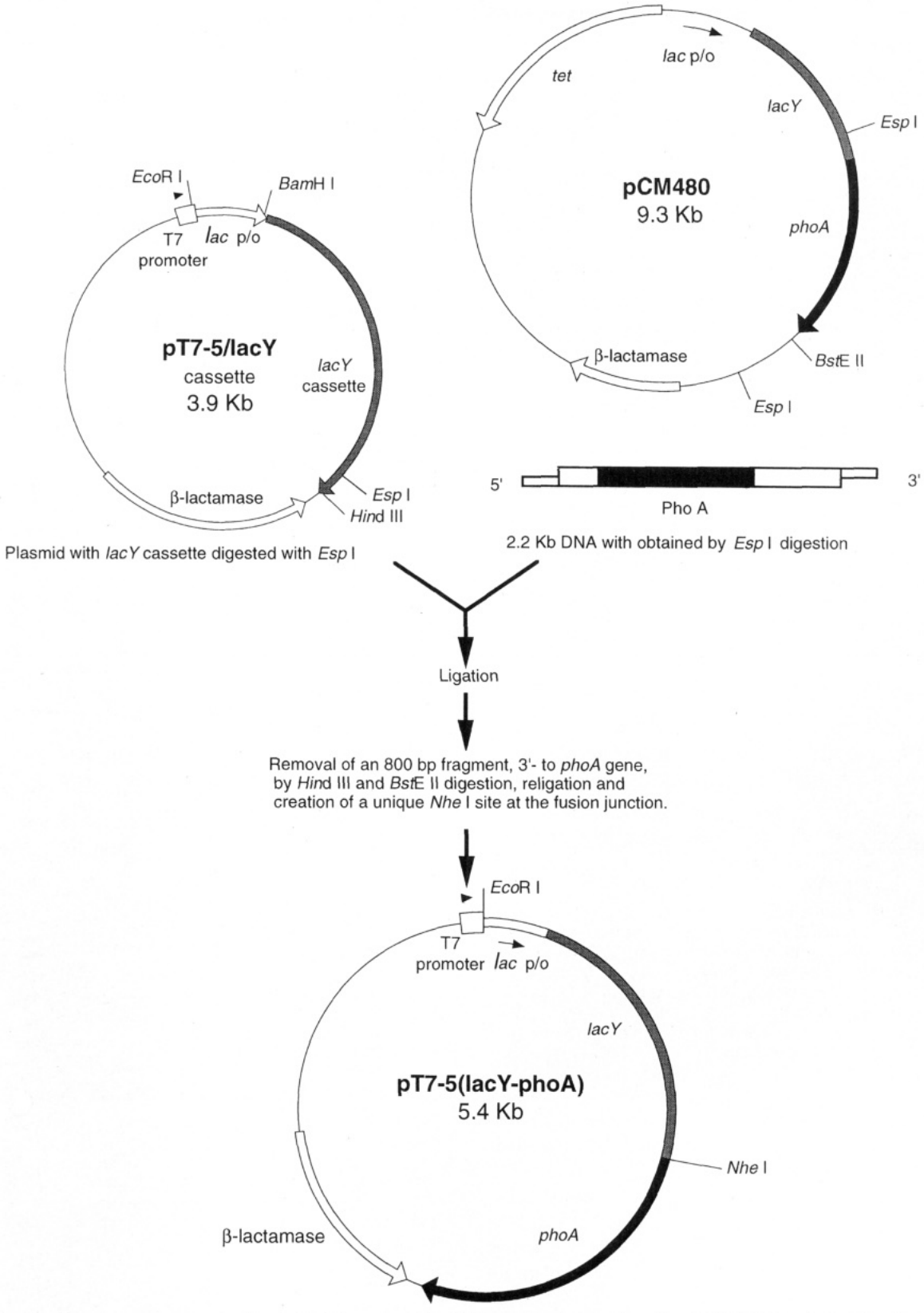


FIGURE 2: Construction of cassette *lacY−phoA* fusion plasmid pT7−5(*lacY−phoA*). Plasmid pCM480 (Calamia & Manoil, 1990) was digested with *Esp*I. The 2.2 kb fragment carrying the *phoA* gene was cloned in the correct orientation into the *Esp*I restriction site of plasmid pT7−5/lacY, yielding plasmid pT7−5(*lacY−phoA*). Plasmid pT7−5(*lacY−phoA*) contains the full length *lacY* gene fused in-frame with the *phoA* gene. Portions of DNA 3′ *phoA* were removed by *Bst*EII and *Hin*dIII digestion. A unique *Nhe*I site is introduced at the junction between *lacY* and *phoA* by two-stage PCR.

results demonstrate that the high-activity fusions have higher specific activities. The stabilities of Phe220-PhoA, a representative low-activity construct, and of Asp240-PhoA, a representative high-activity construct, were examined by pulse−chase experiments (data not shown). The fusion proteins were identified by immunoprecipitation with anti-BAP at each time point during the chase, and it is apparent that both fusions are stable during the entire 3-h chase period.

Table 1: DNA Sequence Analysis of *lacY−phoA* Gene Fusions

| fusion primer | oligonucleotide sequence[a,b,c,d] |
|---|---|
| L216-Pho A | 5′-AGAGTCGCTAGC**CAG**TTCCAGTGCCAGCTTAAGGC-3′(←) |
| R218-Pho A | 5′-AGAGTCGCTAGC**TCT**GAACAGTTCCAGTGCCAGC-3′(←) |
| P220-Pho A | 5′-GTCGCTAGC**TGG**CTGTCTGAACAGTTCCAGTGCC-3′(←) |
| L222-Pho A | 5′-GTCGCTAGC**CAG**TTTTGGCTGTCTGAACAGTTCCAG-3′(←) |
| F224-Pho A | 5′-GTCGCTAGC**AAA**CCACAGTTTTGGCTGTCTGAACAG-3′(←) |
| S226-Pho A | 5′-GTCGCTAGC**TGA**CAAAAACCACAGTTTTGGCTG-3′(←) |
| Y228-Pho A | 5′-AGAGTCGCTAGC**ATA**CAGTGACAAAAACCACAGTTTTGG-3′(←) |
| I230-Pho A | 5′-AGAGTCGCTAGC**AAT**AACATACAGTGACAAAAACCACAG-3′(←) |
| V232-Pho A | 5′-AGAGTCGCTAGC**AAC**GCCAATAACATACAGTGAC-3′(←) |
| C234-Pho A | 5′-AGAGTCGCTAGC**GCA**GGAAACGCCAATAACATACAGTG-3′(←) |
| T235-Pho A | 5′-GTCGCTAGC**GGT**GCAGGAAACGCCAATAACATACAG-3′(←) |
| Y236-Pho A | 5′-GTCGCTAGC**GTA**GGTGCAGGAAACGCCAATAAC-3′(←) |
| D237-Pho A | 5′-GTCGCTAGC**ATC**GTAGGTGCAGGAAACGCC-3′(←) |
| V238-Pho A | 5′-GTCGCTAGC**AAC**ATCGTAGGTGCAGGAAACGCC-3′(←) |
| D240-Pho A | 5′-AGAGTCGCTAGC**GTC**AAAAACATCGTAGGTGCAGGAAACGCC-3′(←) |
| F243-Pho A | 5′-GTCGCTAGC**AAA**CTGTTGGTCAAAAACATCGTAGG-3′(←) |
| F247-Pho A | 5′-GTCGCTAGC**AAA**GAAATTAGCAAACTGTTGGTC-3′(←) |
| F250-Pho A | 5′-AGAGTCGCTAGC**GAA**CGAAGTAAAGAAATTAGCAAACTGTTG-3′(←) |
| A252-Pho A | 5′-AGAGTCGCTAGC**AGC**AAAGAACGAAGTAAAGAAATTAGC-3′(←) |
| G254-Pho A | 5′-AGAGTCGCTAGC**ACC**GGTAGCAAAGAACGAAGTAAAGAAATTAGC-3′(←) |
| V352-Pho A | 5′-AGAGTCGCTAGC**GAC**CAGATAAATCGTCGCTGAAAAACGC-3′(←) |
| F354-Pho A | 5′-AGAGTCGCTAGC**GAA**ACAGACCAGATAAATCGTCGCTGAAAAACGC-3′(←) |
| F356-Pho A | 5′-AGAGTCGCTAGC**GAA**GCAGAAACAGACCAGATAAATCGTCGC-3′(←) |
| F357-Pho A | 5′-AGAGTCGCTAGC**AAA**GAAGCAGAAACAGACCAGATAAATCGTCGC-3′(←) |
| K358-Pho A | 5′-AGAGTCGCTAGC**CTT**AAAGAAGCAGAAACAGACCAG-3′(←) |
| Y373-Pho A | 5′-AGAGTCGCTAGC**ATA**CATATTGCCCGCCAGTACAGAC-3′(←) |

[a] Underlined nucleotides indicate the unique recognition sequence for *Nhe*I at the fusion junction. [b] Boldfaced triplet indicates the last amino acid of *lac* permease at the fusion junction. [c] Arrow denotes antisense oligo (←). [d] Unique *Nhe*I site was created at the junction of full-length *lacY−phoA* construct by introducing a silent mutation on the first codon of the *phoA* gene.

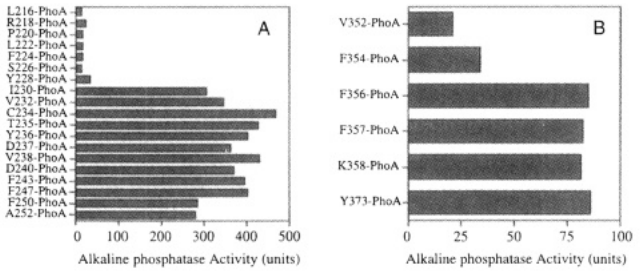


FIGURE 3: Alkaline phosphatase activity of *lacY−phoA* gene fusions in helices VII (A) and XI (B). Alkaline phosphatase activity was assayed by measuring the rate of hydrolysis of *p*-nitrophenyl phosphate at 480 nm by permeabilized CC181 cells expressing *lacY−phoA* fusions as described under Experimental Procedures. Fusions are characterized by the single-letter amino acid code of the C-terminal amino acid of the *lacY* fragments followed by a number indicating the position of the residue in wild-type permease and *-phoA*.

*Periplasmic Alkaline Phosphatase.* In order to test the ability of N-terminal transmembrane segments of lac permease to promote export of alkaline phosphatase, periplasmic proteins from cells expressing *lacY−phoA* fusions in transmembrane domain VII were isolated and subjected to Western blot analysis using anti-BAP (Figure 5). Bands corresponding to native alkaline phosphatase (47.5 kDa) are observed in the periplasmic fraction from cells expressing the fusions, and the intensity of the bands is correlated with the activity of the fusions (compare Figures 5 and 3A). The observations indicate that, to an extent, the N-terminal lac permease portion of the active chimeras behaves like a signal sequence, promoting export and release of alkaline phosphatase into the periplasm. It is also noteworthy, however, that substantial portions of the chimeric proteins remain associated with the membrane as indicated by Western blots of the membrane fraction (data not shown).

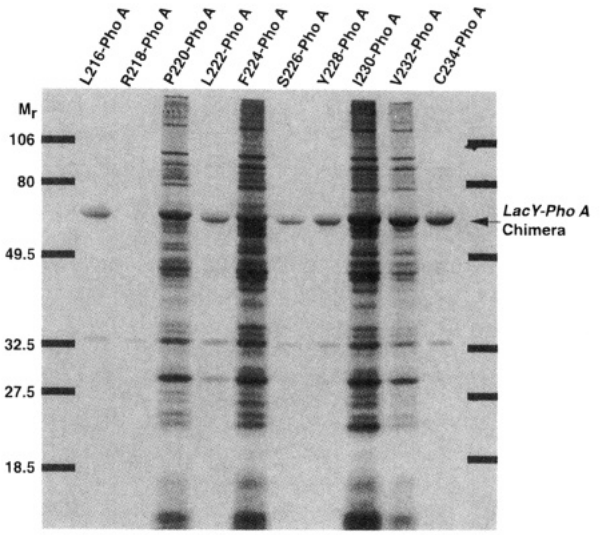


FIGURE 4: Immunoprecipitation of *lacY−phoA* fusion proteins. Aliquots of IPTG-induced *E. coli* CC181 ($7 \times 10^8$ cells) were labeled with [$^{35}$S]methionine at 37 °C for 5 min. The labeled fusion proteins were immunoprecipitated with anti-BAP and subjected to SDS−PAGE. The positions of the molecular weight markers are indicated. The amount of fusion protein was quantitated by Phosphor Imaging (Table 2).

*Site-Directed Fluorescence Quenching.* The location of residues Asp237 (helix VII) and Lys358 (helix XI) relative to the surface of the membrane was also studied by fluorescence quenching using PM-labeled single-Cys mutants D237C/K358A and D237A/K358C. These double mutants were selected since the simultaneous replacement of Asp237 and Lys358 with this combination of neutral amino acid residues yields active, single-Cys permeases (Dunten et al., 1993). Acrylamide was used as a water-soluble quencher, and 5-doxylstearic acid or 12-doxylstearic acid served as lipid-soluble quenchers. Fluorescence quenching of both

Table 2: Specific Activities of *lacY−phoA* Fusions

| *lacY−phoA* chimera | relative protein synthesis[a] | specific activity[b] |
|---|---|---|
| L216-Pho A | 1.0 | 12.1 |
| R218-Pho A | 0.5 | 40.0 |
| P220-Pho A | 3.0 | 4.6 |
| L222-Pho A | 1.0 | 13.9 |
| F224-Pho A | 4.0 | 2.8 |
| S226-Pho A | 0.8 | 15.3 |
| Y228-Pho A | 1.1 | 25.8 |
| I230-Pho A | 4.9 | 54.5 |
| V232-Pho A | 2.4 | 124.7 |
| C234-Pho A | 1.5 | 272.4 |

[a] Relative rates were measured by quantitating the amount of labeled protein in each independent chimeric construct by using a Phospor Imager (Molecular Dynamics). The *lacY−phoA* chimera was arbitrarily set at 1.0. [b] Specific activities were measured by dividing the alkaline phosphatase activity by the relative amount of protein synthesized, under identical conditions of induction. Specific activities were normalized for cell densities, both for assaying alkaline phosphatase activity and for their corresponding rate of protein synthesis.

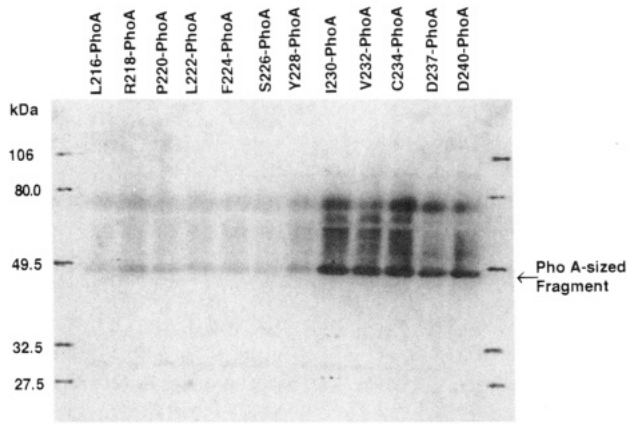


FIGURE 5: Western blots of periplasmic proteins. Equal amounts of periplasmic protein (35 $\mu$g) prepared from *E. coli* CC181 expressing individual *lacY−phoA* fusions as described under Experimental Procedures were subjected to 12% SDS/PAGE and electroblotted. Alkaline phosphatase was detected by reaction with anti-BAP, followed by incubation with [$^{125}$I]protein A and Phosphor Imaging. The intensity of the bands correlates directly to the alkaline phosphatase activity of the fusions.

pyrene-labeled mutants by all three collisional quenchers yields linear Stern−Volmer plots (Figure 6). Strikingly, the fluorescence of pyrene-labeled D237C/K358A and D237A/K358C is efficiently quenched by doxylstearic acids, exhibiting Stern−Volmer constants on the order of $10^4$ $M^{-1}$ (Figure 6, upper panels; Table 3), although pyrene-labeled D237A/K358C is quenched less effectively than D237C/K358A. With both mutants, moreover, 5-doxylstearic acid quenches more efficiently than the 12-doxyl homologue. With acrylamide, a polar quencher, very high concentrations (close to 1.0 M) are required to obtain significant quenching (Figure 6, lower panels). The results clearly indicate that pyrene at position 237 or 358 is in contact with the lipid phase of the membrane. On the other hand, the low but significant quenching of fluorescence observed with acrylamide and the higher quenching efficiency of 5-doxylstearic acid suggest that these positions may be closer to the periplasmic ends of the respective transmembrane helices than to the middle.

*Spin Labeling.* Mutants D237C/K358A and D240C/K319A were also derivatized with methane thiosulfonate spin-label and studied by EPR. Both mutants exhibit similar

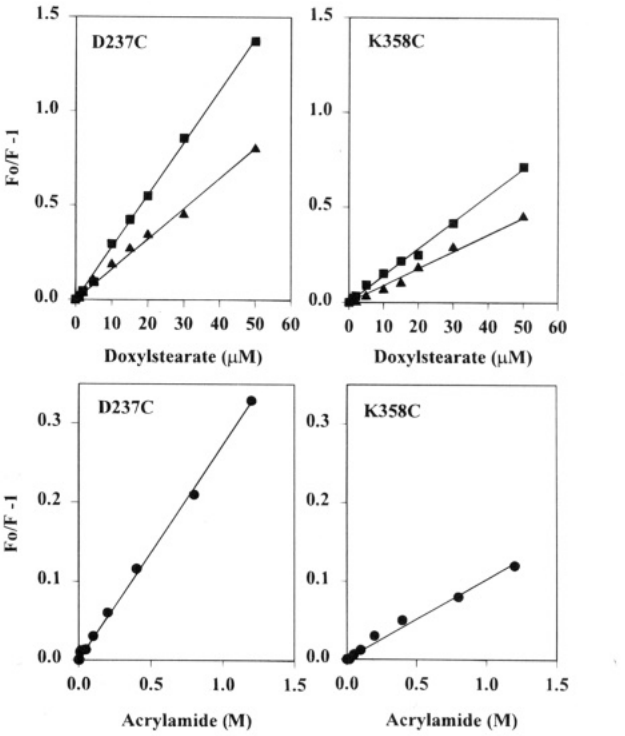


FIGURE 6: Fluorescence quenching of the pyrene-labeled single-Cys mutants D237C/K358A and D237A/K358C by 5-doxylstearic acid (■), 12-doxylstearic acid (▲) and acrylamide (●). Fluorescence was measured at 470 nm in 50 mM $KP_i$ (pH 7.5) at a protein concentration of 35 $\mu$g/mL in the presence of given concentrations of quencher. The excitation wavelength was 344 nm, and the temperature was maintained at 25 °C. Data are presented as Stern−Volmer plots (see Experimental Procedures).

Table 3: Stern−Volmer Constants for the Fluorescence Quenching of Pyrene-Labeled Single-Cys Mutants D237C and K358C[a]

| quencher | Stern−Volmer constant, $K_{SV}$ ($M^{-1}$) | |
|---|---|---|
| | D237C | K358C |
| 5-doxylstearate | $2.8 \times 10^4$ | $1.4 \times 10^4$ |
| 12-doxylstearate | $1.6 \times 10^4$ | $8.9 \times 10^3$ |
| acrylamide | 0.27 | 0.12 |

[a] Protein concentrations: 35 $\mu$g/mL. Values represent the average of three determinations calculated from Stern−Volmer plots such as those shown in Figure 6.

Table 4: Depth of Positions 237 and 240 in the Membrane As Measured by Accessibility to Oxygen or NiAA

| residue | $\Delta P_{1/2}$ (air)[a] | $\Delta P_{1/2}$ (NiAA)[b] | $\phi$[c] | $d$ (Å)[d] |
|---|---|---|---|---|
| 237 | 9.87 | 15.4 | −0.445 | 4.6 |
| 240 | 10.04 | 21.1 | −0.745 | 3.4 |

[a] Microwave power for half-saturation of the EPR signal in samples equilibrated with 21% oxygen at 1 atm. [b] Microwave power for half-saturation of the EPR signal in samples equilibrated with $N_2$ in the presence of NiAA. [c] $\phi = \ln[\Delta P_{1/2}(\text{air})/\Delta P_{1/2}(\text{NiAA})]$. [d] $d$, depth from phosphate head group of the membrane phospholipid.

line shapes (not shown) and accessibility to oxygen or NiAA (Table 4), which is consistent with the notion that this region of the permease is in an α-helical conformation, since both residues would be expected to be on the same face of the helix and therefore in a similar environment.

Due to gradients in solubility, collisions with oxygen increase toward the center of the phospholipid bilayer, while collisions with the polar nickel complex decrease over the same distance. It has been shown (Altenbach et al., 1994)

that the parameter $\Phi = \ln[\Delta P_{1/2}(O_2)/\Delta P_{1/2}(NiAA)]$ is independent of steric features at surface sites in a protein and a linear function of the distance of a nitroxide from the membrane surface. Quantitation of the data indicate that positions 237 and 240 are approximately 5 and 3 Å, respectively, below the phosphate head groups in the membrane (Table 4).

## DISCUSSION

By using *lacY−phoA* fusions in combination with site-directed spectroscopy, we have studied the topology of transmembrane domains VII and XI in lac permease which are thought to be in close proximity, with Asp237 (helix VII) and Lys358 (helix XI) probably forming a salt bridge (King et al., 1991; Sahin-Tóth et al., 1992; Dunten et al., 1993; Sahin-Tóth & Kaback, 1993; Jung et al., 1995; He et al., 1995a,b). The results presented here provide more direct evidence for the suggestion of King et al. [1991; see Zen et al. (1994) in addition] that Asp237 and Asp240 are contained within transmembrane domain VII rather than in the periplasmic loop between helices VII and VIII, as postulated originally from hydropathy analysis (Foster et al., 1983). In addition, the data are consistent with the interpretation that the periplasmic end of transmembrane domain VII is in an α-helical conformation and suggest that Asp237 and Asp240 may be in the periplasmic third of helix VII, rather than in the middle of the transmembrane domain (Figure 1).

Calamia and Manoil (1990) have shown that the alkaline phosphatase activity of *lacY−phoA* fusion proteins engineered at every third amino acid residue in putative helices III and V of lac permease increases abruptly as the fusion junction proceeds from the 8th to the 11th residue, thereby indicating that about half of a transmembrane domain is needed to translocate alkaline phosphatase across the membrane. On the basis of this notion, alkaline phosphatase was fused at alternate amino acid residues in transmembrane helices VII and XI. Alkaline phosphatase activity of cells expressing the chimeras exhibits a sharp increase as the fusion junction is moved from Tyr228 to Ile230 in helix VII, indicating that these residues are located in the approximate middle of the transmembrane domain. Comparison of these results with the secondary structure model of Foster et al. (1983) (Figure 1) suggests that the middle of transmembrane domain VII should be shifted by at least seven amino acid residues toward the N terminus of the permease. Thus, residues Thr235 to Gln241 are transferred from the loop between helices VII and VIII into transmembrane domain VII and residues Leu212 to Phe217 from transmembrane domain VII into the cytoplasmic loop between helices VI and VII. A similar modification was suggested by Zen et al. (1994) based on functional expression of contiguous, nonoverlapping permease fragments. A sharp increase in alkaline phosphatase activity is also observed when the fusion junction is moved from Phe354 to Phe356, placing these residues in the approximate middle of transmembrane domain XI (Figure 1). It is also noteworthy that the fusion approach has been applied to putative transmembrane helices IX and X (M. L. Ujwal, E. Bibi, C. Manoil, and H. R. Kaback, manuscript in preparation). When fusions are constructed at each amino acid residue in these domains, the data are in excellent agreement with the original secondary structure model (Foster et al., 1983).

In order to study the environment of Asp237 and Lys358, which are postulated to form a salt bridge, fluorescence quenching of the appropriate purified and reconstituted pyrene-labeled single-Cys mutants by doxylstearic acids or acrylamide was studied (Figure 6; Table 3). The high efficiency of fluorescence quenching exhibited by the lipid-soluble doxylstearic acids demonstrates clearly that positions 237 and 358 are accessible from the lipid phase and likely therefore to be located within the membrane. This conclusion is in general agreement with the secondary structure model of King et al. (1991) and Zen et al. (1994). Recent data by Abrams and London (1992) propose an interaction distance of 11−15 Å for the quenching of fluorophores by spin-labeled lipids, and the cross section of a transmembrane α-helix including the amino acid side chains is on the order of 10 Å. Therefore, appreciable quenching of the fluorophore by spin-labeled lipids or fatty acids indicates that the fluorophore is located close to the lipid−protein interface (Musser et al., 1993). On the basis of these considerations, the fluorescence quenching results suggest that the regions of transmembrane domains VII and XI containing Asp237 and Asp240 and Lys358, respectively, are located near a surface of the protein that is at least partially in contact with the lipid bilayer rather than buried in the interior of the protein. Furthermore, 5-doxylstearic acid is a more efficient quencher than 12-doxylstearic acid (Figure 6, upper panels). Since the C5 and C12 positions of stearic acid are about 6 and 15 Å, respectively, removed from the carboxyl head group (Voges et al., 1987), the results are consistent with the placement of positions Asp237 and Lys358 near the periplasmic end of transmembrane domains VII and XI, respectively. However, the quenching data do not allow an exact depth determination in the membrane, since it is necessary to know the absolute partition coefficients of the spin-labeled fatty acids and the microviscosity of the bilayer in order to extract more precise information about the proximity between the fluorophore and the quencher (Blatt et al., 1984). Nonetheless, the assignment of Asp237 and Lys358 to positions near the periplasmic ends of the corresponding helices is consistent with the finding that low but significant quenching of pyrene at these positions is observed at high concentrations of acrylamide, a polar collisional quencher (Figure 6, lower panels). On the basis of the assumption that Asp237 and Lys358 form a salt bridge and should therefore be located in the same environment, it would be expected that fluorescence quenching of pyrene at these positions should yield the same properties, and, indeed, the data obtained are similar. Nonetheless, pyrene attached to position 358 appears to be relatively less accessible to the aqueous phase than pyrene at position 237 (Figure 6).

Site-directed spin-labeling of single-Cys mutants D237C and D240C was also employed to investigate the environment surrounding these positions. Analysis of collision-induced $T_{1e}$ relaxation of nitroxide spin-labels at these positions by apolar molecular oxygen or hydrophilic NiAA (Altenbach et al., 1994) yields distances of 5 and 3 Å below the phospholipid head groups for positions 237 and 240, respectively, indicating that both residues are relatively close to the end of the helix. In addition, the distances are consistent with an α-helical conformation in this region of transmembrane domain VII.

Finally, it should be noted that the results are also consistent with the possibility that helices VII and XI line

the solvent-filled notch that has been observed in the permease (Costello et al., 1984, 1987; Li & Tooth, 1987). Localization of hydrophilic faces of amphipathic helices in the cleft could also account for the accessibility of the covalently attached spectroscopic probes to hydrophilic quenchers. In any case, the data presented here taken together with the findings of Zen et al. (1994) provide direct support for the argument that Asp237, Asp240, and Lys358 are located within transmembrane helices in lac permease.

## REFERENCES


Abrams, F. S., & London, E. (1992) *Biochemistry 31*, 5312.
Altenbach, C., Flitsch, S. L., Khorana, H. G., & Hubbell, W. L. (1989) *Biochemistry 28*, 7806.
Altenbach, C., Greenhalgh, D. A., Khorana, H. G., & Hubbell, W. L. (1994) *Proc. Natl. Acad. Sci. U.S.A. 91*, 1667.
Blatt, E., Chatelier, R. C., & Sawyer, W. H. (1984) *Photochem. Photobiol. 39*, 477.
Calamia, J., & Manoil, C. (1990) *Proc. Natl. Acad. Sci. U.S.A. 87*, 4937.
Consler, T. G., Persson, B. L., Jung, H., Zen, K. H., Jung, K., Privé, G. G., Verner, G. E., & Kaback, H. R. (1993) *Proc. Natl. Acad. Sci. U.S.A. 90*, 6934.
Costello, M. J., Viitanen, P. V., Carrasco, N., Foster, D. L., & Kaback, H. R. (1984) *J. Biol. Chem. 259*, 15570.
Costello, M. J., Escaig, J., Matsushita, K., Viitanen, P. V., Menick, D. R., & Kaback, H. R. (1987) *J. Biol. Chem. 262*, 17072.
Dunten, R. L., Sahin-Tóth, M., & Kaback, H. R. (1993) *Biochemistry 32*, 3139.
Foster, D. L., Boublik, M., & Kaback, H. R. (1983) *J. Biol. Chem. 258*, 31.
He, M., Voss, J., Hubbell, W. L., & Kaback, H. R. (1995a) *Biochemistry* (in press).
He, M., Voss, J., Hubbell, W. L., & Kaback, H. R. (1995b) *Biochemistry* (in press).
Ho, S. N., Hunt, H. D., Horton, R. M., Pullen, J. K., & Pease, L. R. (1989) *Gene 77*, 51.
Ito, K., Bassford, P., & Beckwith, J. (1981) *Cell 24*, 707.
Jung, K., Jung, H., Wu, J., Privé, G. G., & Kaback, H. R. (1993) *Biochemistry 32*, 12273.
Jung, K., Jung, H., & Kaback H. R. (1994) *Biochemistry 33*, 3980.
Jung, K., Voss, J., He, M., Hubbell, W. L., & Kaback, H. R. (1995) *Biochemistry 34*, 6272.
Kaback, H. R. (1989) *Harvey Lect. 83*, 77.
Kaback, H. R. (1992) *Int. Rev. Cytol. 137A*, 97−125.
Kaback, H. R., Jung, K., Jung, H., Wu, J., Privé, G. G., & Zen, K. H. (1993) *J. Bioenerg. Biomembr. 25*, 627.
Kaback, H. R., Frillingos, S., Jung, H., Jung, K., Privé, G. G., Ujwal, M. L., Weitzman, C., Wu, J., & Zen, K. (1994) *J. Exp. Biol. 196*, 183.
King, S. C., Hansen, C. L., & Wilson, T. H. (1991) *Biochim. Biophys. Acta 1062*, 177.
Kouyama, T., & Mihashi, K. (1981) *Eur. J. Biochem. 114*, 33.
Laemmli, U. K. (1970) *Nature (London) 227*, 680.
Lee, J.-I., Hwang, P. P., Hansen, C., & Wilson, T. H. (1992) *J. Biol. Chem. 267*, 20758.
Li, J., & Tooth, P. (1987) *Biochemistry 26*, 4816.
Manoil, C., & Beckwith, J. (1985) *Proc. Natl. Acad. Sci. U.S.A. 82*, 8129.
Musser, S. M., Larsen, R. W., & Chan, S. I. (1993) *Biophys. J. 65*, 2348.
Sahin-Tóth, M., & Kaback, H. R. (1993) *Biochemistry 32*, 10027.
Sahin-Tóth, M., Dunten, R. L., Gonzalez, A., & Kaback, H. R. (1992) *Proc. Natl. Acad. Sci. U.S.A. 89*, 10547.
Sahin-Tóth, M., Lawrence, M., & Kaback, H. R. (1994) *Proc. Natl. Acad. Sci. U.S.A. 91*, 5421.
Sanger, F., Nicklen, S., & Coulsen, A. R. (1977) *Proc. Natl. Acad. Sci. U.S.A. 74*, 5463.
Schaffner, W., & Weissmann, C. (1973) *Anal. Biochem. 56*, 502.
Tabor, S., & Richardson, C. C. (1985) *Proc. Natl. Acad. Sci. U.S.A. 82*, 1074.
Teather, R. M., Bramhall, J., Riede, I., Wright, J. K., Fürst, M., Aichele, G., Wilhelm, V., & Overath, P. (1980) *Eur. J. Biochem. 108*, 223.
van Iwaarden, P. R., Pastore, J. C., Konings, W. N., & Kaback, H. R. (1991) *Biochemistry 30*, 9595.
Viitanen, P. V., Newman, M. J., Foster, D. L., Wilson, T. H., & Kaback H. R. (1986) *Methods Enzymol. 125*, 429.
Voges, K.-P., Jung, G., & Sawyer, W. H. (1987) *Biochim. Biophys. Acta 896*, 64.
Zen, K. H., McKenna, E., Bibi, E., Hardy, D., & Kaback, H. R. (1994) *Biochemistry 33*, 8198.


BI9517300